Supporting Information

Regulation of Heterogeneous Electron Transfer Reactivity by Defect Engineering through Electrochemically Induced Brominating Addition

Lanping Zeng, [a,c] Lianhuan Han, [*b] Wenjing Nan, [a] Weiying Song, [a] Shiyi Luo, [a] Yuan-Fei Wu, [a] Jian-Jia Su, [a] Dongping Zhan[a]

a State Key Laboratory of Physical Chemistry of Solid Surfaces (PCOSS), Engineering Research Center of Electrochemical Technologies of Ministry of Education, Department of Chemistry, College of Chemistry and Chemical Engineering, Xiamen University, Xiamen 361005, China.

b Department of Mechanical and Electrical Engineering, Pen-Tung Sah Institute of Micro-Nano Science and Technology, Xiamen University, Xiamen 361005, China.

c Fujian Science & Technology Innovation Laboratory for Energy Materials of China (Tan Kah Kee Innovation Laboratory), Xiamen 361005, China

S1. The XPS characterization of brominated graphene.

XPS experiments were performed to identify the carbon-bromine (C-Br) functionalization of the SLG surface. As shown in Fig. S1a, the characteristic photoelectrons peaks of C 1s, O1s and Si elements are clearly observed. The peaks at 103 eV (Si 2p) and 154 eV (Si 2s) are related to the SiO_2 /Si substrate. In the case of brominated graphene (SLGBr), new characteristic peaks appeared due to the brominating process, which are attributed to the Br 3s at 257 eV, Br 3p at 183 eV and Br 3d at 70 eV , respectively. High-resolution XPS spectrum for Br 3d signal is shown in Fig. S1b. The Br 3d peak can be fitted into a pair of peaks at 70.3 eV and 71.3 eV, which is caused by the spin orbit splitting of that leads to a doublet structure Br $3d_{5/2}$ and Br $3d_{3/2}$. This signal indicates the formation of covalent C-Br bond. A weak XPS peak is observed at about 68.5 eV, which might be due to trace amount of adsorbed Br^- . All the above results demonstrate the occurrence of an electrochemically induced brominating addition reaction and that the SLG can be brominated to form SLGBr.

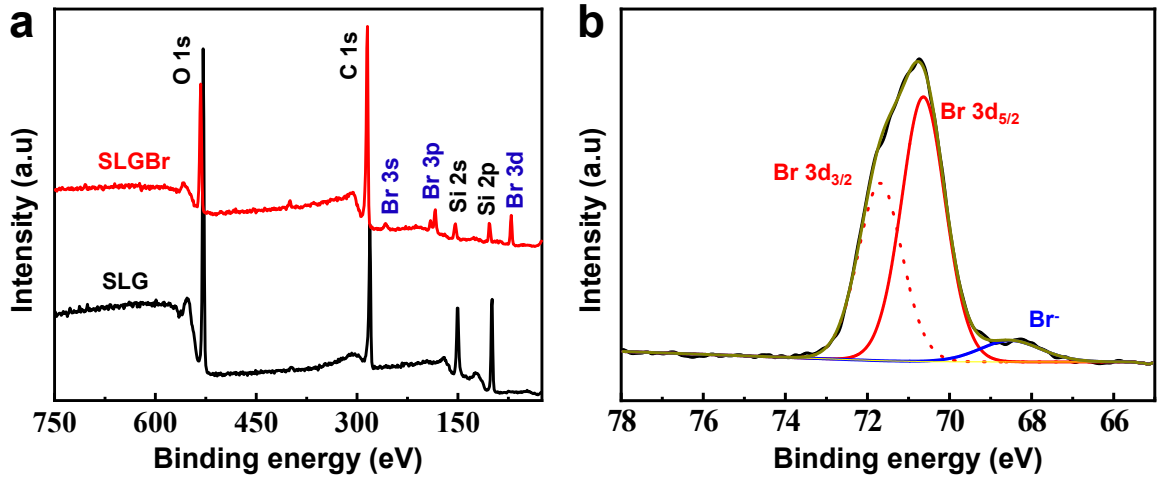

Fig. S1 (a) XPS spectrum of SLG and SLGBr before and after bromination. (b) High resolution XPS spectrum of Br 3d

S2. Determination of the defect density of graphene by Raman spectroscopy.

The value of C_A in equation (1) in the main text is dependent on the excitation energy, and will also influence the maximum possible value of I_D/I_G (Fig. S2) and, consequently, the deduced mean distance between defects (L_D). According to the literature, the dependence of C_A on the excitation energy (E_L, eV) is illustrated by $C_A = (160 \pm 48)\ E_L^{-4}$. Considering the excitation laser of 532 nm (2.33 eV) in our experiment, we can obtain $C_A = 5.43 \pm 1.63$. Using the average, lower and upper limit values of C_A (i.e., 3.8, 5.4 and 7.1, respectively), we can plot the dependence of I_D/I_G on L_D, as shown in Fig. S2. It can be clearly seen from the plot that the scattering of the values of C_A (5.43 ± 1.63) is large, the most appropriate value of C_A can be deduced from the maximum possible value of I_D/I_G. For large amounts of data of Raman spectra of graphene with different defect densities we tested, the maximum value of I_D/I_G is about 3.2, which agrees well with that using $C_A = 4.2$ at similar green line excitation (514 nm, 2.41 eV). Therefore, we used $C_A = 4.2$ in equation (1) to deduce the defect density of graphene (the blue line).

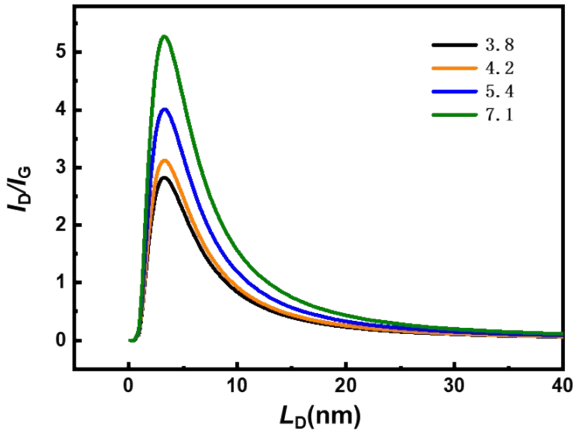

Fig. S2. The fitted $I_D/I_G \sim L_D$ curves by equation (1) in the main text with different values of C_A, r_S = 1 nm，r_A = 3 nm.

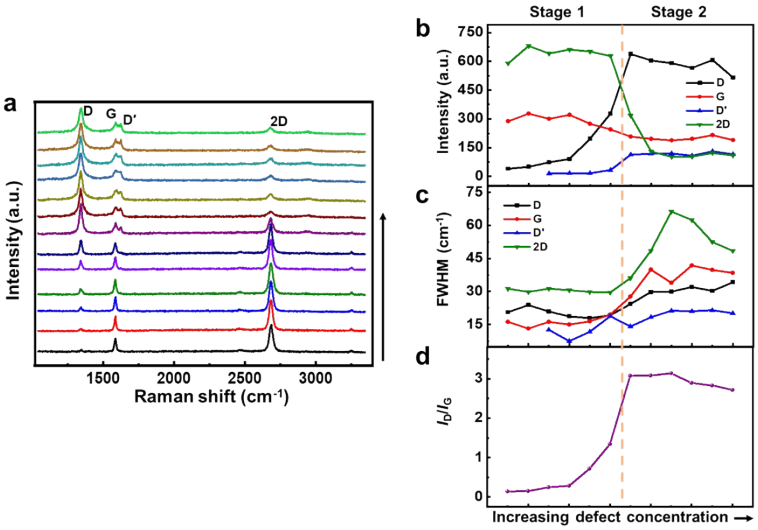

Fig. S3. (a) The Raman spectra of graphene with different defect densities on a single graphene sheet. The arrow indicates the increasing of the defect density. Evolution of Raman intensity (b) and full width at half maximum (FWHM) (c) of the D, G, D' and 2D peaks with increasing defect density. (d) The corresponding I_D/I_G for graphene samples with increasing defect density. The results show a two-stage evolution as discussed in main text. The two-stage change of Raman spectra could be discriminated by the FWHM of the bands. When the defect density reaches Stage 2, all the Raman bands start to broaden.

S3. The schematic diagram of the SECM

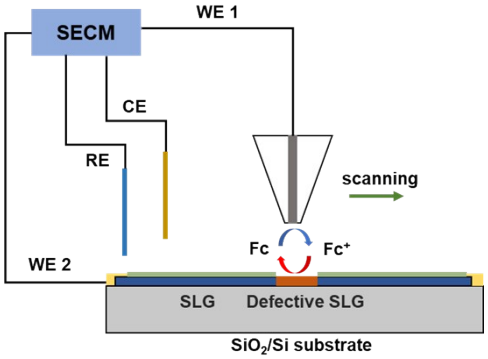

Fig. S4. The schematic diagram of the setup for SECM imaging of defective graphene samples. The graphene substrate was

used as the substrate electrode (WE 2) and kept unbiased during the experiment. A 5-μm radius (r) Pt ultramicroelectrode UME (RG = 2) was placed over the graphene substrate used as the working electrode (WE 1), the UME tip was held at 0.45 V vs Ag/AgCl to ensure the electrode reaction under a diffusion-limited condition. A platinum wire was served as the counter electrode and an Ag/AgCl electrode as the reference electrode. The electrolyte used here was 1 mM FcMeOH + 0.1 M KCl aqueous solution. By scanning over the graphene sample surface, one can spatially image the local electrochemical activity at different positions.

S4. Finite element method (FEM) modeling

To quantify the HET rate of the graphene samples, FEM modeling was used to simulate the tip current response as a function of k^0 through COMSOL Multiphysics 5.5 (COMSOL AB, Sweden). The time-dependent mass transport in solution for axisymmetric cylindrical coordinates is governed by equation (S1):

$$\frac{\partial C_i}{\partial t} = D_i \nabla^2 C_i \quad \text{(S1)}$$

where C_i (mol/cm^3) and D_i (cm^2/s) represent the concentration and diffusion coefficient of the FcMeOH species in solution, respectively. The diffusion coefficient of the FcMeOH species here is 7.4×10^{-6} cm^2 s^{-1}.The geometry for finite element model is displayed in Fig. S5, where a is the radius of the Pt wire, d is the distance between the tip and the substrate electrode. The simulations were carried out with RG = 2. The numbers in Fig. S5 represent the boundaries as defined in Table S1.

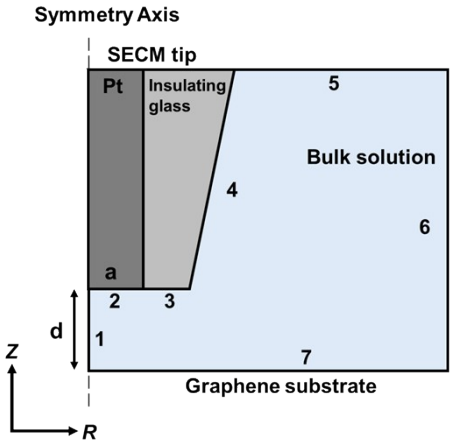

Fig. S5. The schematic diagram of the axisymmetric cylindrical geometry used for the simulation of the feedback mode. The numbers represent the boundary numbers as defined in Table S1.

Table S 1 A summary of the boundary conditions used in feedback mode to determine k^0 of graphene.

Lable in Fig. S5	Boundary type	Equation
1	Axis of symmetry/insulation	$\nabla C_i \cdot \vec{n} = 0$

2	Pt UME/concentration	$C_{FcMeOH} = 0,\ C_{FcMeOH+} = C^{b}_{FcMeOH}$
3, 4	Glass shear/insulation	$\nabla C_i \cdot \vec{n} = 0$
5, 6	Bulk solution/concentration	$C_{FcMeOH} = C^{b}_{FcMeOH},\ C_{FcMeOH+} = 0$
7	Graphene surface/flux	$-D_{FcMeOH+}\nabla C_{FcMeOH+} \cdot \vec{n} = k^0 C_{FcMeOH+}$ $-D_{FcMeOH}\nabla C_{FcMeOH} \cdot \vec{n} = -k^0 C_{FcMeOH+}$

In Table S1, on the axis of symmetry or insulation boundaries 1, 3 and 4, there is no flux normal to the boundaries for all species. $\vec{n}$ is the inward unit vector normal to the surface. On boundary 2, the oxidation of FcMeOH on the Pt tip is under the diffusion-limited condition, C^{b}_{FcMeOH} is the bulk concentration of FcMeOH. On boundaries 5 and 6, the concentration of all species is equal to the bulk solution. On boundary 7 (graphene surface), the $\vec{n}$ of FcMeOH/FcMeOH+ species on this boundary is related to the HET rate of the graphene surface, the boundary condition is defined as shown in Table S1. The tip current is calculated through integrating the flux at the tip surface:

$$i_{tip} = \int_0^a nFD_{FcMeOH}\frac{\partial C_{FcMeOH}}{\partial Z}2\pi R dR \quad \text{(S2)}$$

A series of simulations were carried out by varying the k^0 and d systematically. The corresponding current feedback curves were obtained with different k^0 as shown in Fig. S6. The quantitative kinetics of HET on graphene could be obtained by fitting the experimental feedback curves to the simulations.

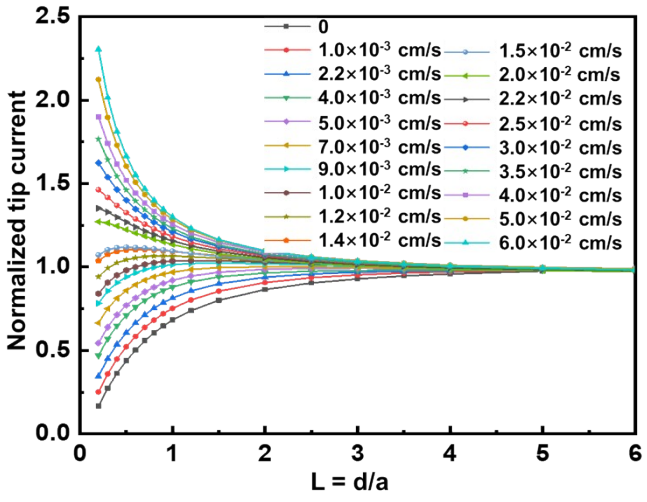

Fig. S6. The simulated feedback curves with different values of k^0, the radius of the SECM tip was 5 μm, RG = 2.

S5. Raman and SECM results on defective graphene patterns

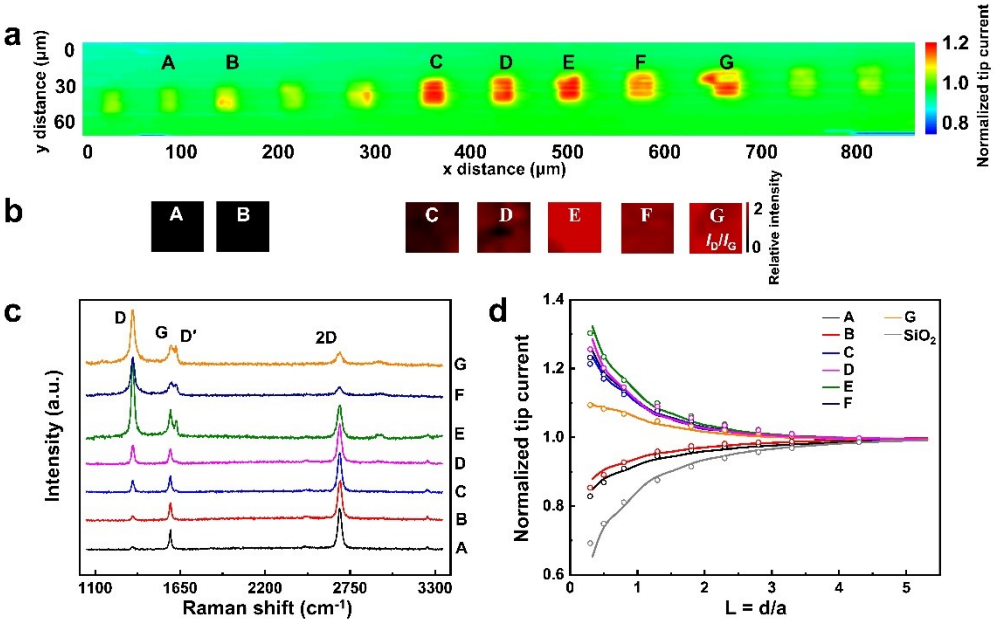

Fig. S7 Additional Raman and SECM results on other sets of defective graphene patterns. (a) SECM images of areas of different defective densities on a SLG sheet. (b) The Ramaning mapping of the D band (I_D/I_G) of the areas of different defective densities with the same scale bar. (c) The correspongding Raman spectra of different areas. (d) The SECM feedback curves obtained on each defective graphene pattern, the solid lines and circles represent the experimental data and simulated results, respectively. The grey line represents the feedback curve obtained on SiO_2 region, and the grey circle represents the totally negative feedback curve when k^0 is zero.